Academic Journal of Science and Technology
ISSN: 2771-3032 | Vol. 17, No. 2, 2025

Simulation and Analysis of the Thermal Environment in Railway Freight Containers under Solar Radiation on the Western Plateau

Zhide Ma

Freight Transport Department, China Railway Lanzhou Group, Huining Gansu, 730700, China

Abstract: Based on the development of railway dangerous goods transportation under the Belt and Road Initiative, this study focuses on the impact of solar radiation on containers and the internal cargo temperature in the western plateau regions. A physical model of a 20-foot universal container was developed. Utilizing SolidWorks and ANSYS for modeling and meshing, a mathematical model incorporating heat conduction, convection, and thermal radiation was constructed. By introducing a solar load model and the S2S (surface-to-surface) radiation method, the temperature variation process under typical daytime conditions in Lanzhou City was simulated.

Keywords: Northwest China; Solar Radiation; Simulation; Container.

1. Introduction

With the advancement of the Belt and Road Initiative and the China-Europe Railway Express, the transport of railway dangerous goods now spans various fields including transportation, medical science, and national defense technology. China's vast territory, stretching thousands of kilometers from east to west and north to south, is now largely covered by a comprehensive railway network, enabling the containerized transport of dangerous goods across most regions. Furthermore, both the variety and volume of railway dangerous goods transport continue to grow—increasing by 5.9% in 2023 and 2.9% in 2024. However, this growth in volume is accompanied by a corresponding rise in safety risks [1]. The State Council's Outline of the 14th Five-Year Plan for Modern Integrated Transportation System emphasizes balanced development of passenger and freight transport, a dual focus on new construction and renovation, and coordinated advancement of high-speed and conventional railways. It calls for accelerating the construction of conventional railways and capacity expansion of existing lines, eliminating bottlenecks in trunk routes, enhancing capacity in congested sections, and improving railway network coverage in central and western regions [2]. This necessitates greater attention to the transport process of railway dangerous goods and higher technical standards for their carriage. Ensuring transport safety while increasing the volume of railway dangerous goods has become an urgent issue to address. Although China's railway network density is already relatively high, coverage in the western regions remains sparse. Only by establishing a more comprehensive network can the overall transport capacity for railway dangerous goods be enhanced to meet current societal demands.

2. Literature References

Wang Chunsheng and Teng Shuai et al. [3], based on typical climatic conditions and using the most severe operating scenario as the boundary, systematically simulated the temperature distribution characteristics of the cargo and container during transport. Their work provides an important reference for the thermal safety assessment and transport condition specification of dangerous goods containers. Wei Yan [4] conducted systematic numerical simulations focusing on the heat transfer behavior of dangerous goods containers under complex external climatic conditions, revealing the temperature response patterns of the container under different thermal boundary conditions. Ling Dechao [5] focused on the thermal environmental characteristics of maritime dangerous goods containers under various practical operating conditions, providing directional guidance for understanding the cumulative effects and control strategies of radiative heat load throughout the container's entire transport journey. Zou Nan [6], by developing a container temperature field model, pointed out that thermal load exerts a non-negligible regulatory effect on structural mechanical behavior. Li Wuliu [7], addressing the transport safety of bulk sulfur in dry bulk containers during high-temperature seasons, provided a basis for container selection and thermal safety prevention for specific cargoes under extreme climate conditions. Zhang Lichun [8] performed thermal experiments on the solar radiation absorptivity of vehicle profile materials. The results indicated that the surface coating significantly affects the absorptivity, while the angle of incidence has a minor influence. The internal structure of the profile and the intensity of radiation showed no significant effect on the absorptivity. Liu Shutang [9] concluded that the solar radiation coefficient has a considerable impact on the temperature of sun-exposed surfaces of steel box-section members. Conversely, the surface convective heat transfer coefficient significantly affects the temperature of these members; in natural environments, this coefficient is primarily influenced by wind speed. Lin Cuocuo [10] employed CFD numerical simulation to model the temperature field of steel structural members and validated the results against experimental data. The analysis identified solar radiation intensity, ambient temperature, and wind speed as major factors influencing the temperature of steel structural members. Guo Zhipeng et al. [11], considering air convection heat transfer and external heat transfer to the container, concluded that leaving a certain gap between cargo units can effectively enhance heat exchange and improve the overall

temperature uniformity inside the container.

3. Model

3.1. Physical Model

Most goods are transported using standard containers; therefore, a 20ft general-purpose container was selected as the research subject. According to international standards, the external dimensions of a 20ft universal container are 6058mm × 2438mm × 2591mm, with internal dimensions of 5898mm × 2352mm × 2393mm. The container structure is constructed using weathering steel.

The model was created in SolidWorks and subsequently imported into ANSYS for meshing. The average mesh element quality achieved was 0.2, indicating excellent mesh quality.

3.2. Mathematical Model.

Governing Equation for Heat Conduction:

$$q = -\lambda \cdot \nabla T \tag{1}$$

Newton's Law of Cooling: Convective Heat Transfer

$$\varphi = \alpha(t_f - t_w)F \tag{2}$$

Thermal Radiation:

Thermal radiation is a mode of energy transfer via electromagnetic waves. This form of heat transfer covers a specific portion of the electromagnetic spectrum, with wavelengths ranging from 0.1 to 100 micrometers. For semi-transparent media (such as glass or combustion product gases), radiation is a volumetric phenomenon because radiation energy can escape from within the bulk of the material itself. For opaque objects, radiation is predominantly a surface phenomenon because nearly all internal radiation is absorbed within the material before it can escape.

$$q_{rad} = \sigma\varepsilon(T_{max}^4 - T_{min}^4) \tag{3}$$

$$q_{conv} = h(T_{wall} - T_{bulk}) \tag{4}$$

Solar Radiative Heat Transfer on Opaque Walls

Solar Irradiance R_1:

$$R_1 = R_{SC}\left[1 + 0.033\cos\frac{360n}{365}\right] \tag{5}$$

Calculation Formula for Direct Solar Transmittance in Clear Sky Conditions:

$$\tau_a = \frac{G_{ST}}{R_1} = a_0 + a_1 e^{\frac{-k}{\sin\beta}} \tag{6}$$

$$a_0 = r_0 a_0^*,\ a_0^* = 0.4237 - 0.00821(6 - A)^2 \tag{7}$$

$$a_1 = r_1 a_1^*, a_1^* = 0.5055 - 0.00595(6.5 - A)^2 \tag{8}$$

$$k = r_k k^*, k^* = 0.2711 - 0.01858(2.5 - A)^2 \tag{9}$$

Direct Solar Radiation Incident on a Horizontal Surface:

$$R_h = R_1 \tau_b \sin h \tag{10}$$

Direct Solar Radiation Incident on a Vertical Surface

$$R_v = R_1 \tau_b \cos h \cos n \tag{11}$$

Sky Diffuse Radiation: Diffuse Solar Radiation Incident on a Horizontal Surface under Clear Sky Conditions

$$R_{SK} = 0.39 R_1 \sin h\left(1 - e^{-\frac{K}{\sin h}}\right) \tag{12}$$

Sky Diffuse Radiation Incident on a Horizontal Surface under Clear Sky Conditions

$$R_{DS} = \frac{R_{SK}}{2} \tag{13}$$

Ground-Reflected Radiation

Since the cargo wagon underbody is not in direct contact with the ground, the radiation reflected from the ground must be considered for the thermal analysis of the underside surfaces.

$$R_{G\theta} = \rho_1(R_{DN}\sin h + R_{SK})\left(1 - \frac{\cos\theta^2}{2}\right) \tag{14}$$

Solar Heat Transfer through Container Exterior Walls

The solar heat flux entering through the exterior walls of the container is calculated using the following equation:

$$\varphi = \alpha \cdot A \cdot \frac{i}{i_w} \cdot B \tag{15}$$

4. Boundary Conditions and Setup

Inlet Boundary Condition Setup:

At the inlet boundary named "inlet," the air supply velocity was set to 0 m/s, and the temperature was set to 25 °C.

Outlet Boundary Condition Setup:

The outlet was defined as a pressure-outlet with a constant gauge pressure of 0 Pa. Backflow conditions were disabled to ensure solution stability.

Wall Boundary Conditions: Thermal Model:

Thermal Model: All walls were configured as coupled thermal boundaries for conjugate heat transfer analysis.

Initial Temperature: A uniform initial temperature of 25°C was applied to all solid domains.

Surface Emissivity: The external walls were assigned an emissivity of 0.73, while the surfaces of the internal goods were set to 0.70.

Gravity Condition:

A gravitational acceleration of 9.81 m/s² was applied along the negative Y-axis to account for natural convection effects.

Ambient Conditions:

Reference Temperature: The ambient temperature was set to 25°C, corresponding to the recorded weather data for Lanzhou at 09:00 AM.

Convective Heat Transfer: An external convective heat transfer coefficient of 5 W/m²·K (typical for natural convection) was applied to exposed surfaces.

Solar Radiation Model:

Methodology: The Solar Ray Tracing (S2S) model was activated to simulate radiative heat transfer.

Geographical Parameters: The simulation was configured for Lanzhou (Longitude: 103.73°, Latitude: 36.03°) with solar positioning calculated for the target time.

Solar Load Components:

Direct Solar Irradiance: 744.649 W/m²

Diffuse Solar Irradiance (Vertical Surface): 112.141 W/m²

Diffuse Solar Irradiance (Horizontal Surface): 98.2456 W/m²

Ground-Reflected Radiation: 49.8058 W/m²

5. Analysis of Simulation Results

The simulation results indicate that at 09:00 AM, the maximum temperature recorded was 30.67°C. The elevated temperatures were primarily concentrated on the eastern and east-northwestern sides of the container, with the eastern side reaching approximately 29°C. The hottest spot was located at a corner region. As the sun's position shifted and solar intensity increased, by 10:00 AM, the maximum temperature rose to 40.34°C. The temperature of the eastern wall reached around 33°C, while both the eastern and western walls registered temperatures near 34°C.At noon (12:00 PM), the peak temperature further increased to 42.19°C. The temperatures of the eastern and western walls were about 37°C, and the eastern side stabilized near 32°C. The

maximum temperature continued to rise until approximately 17:00 (5:00 PM), reaching 45.52°C, with the hottest zones concentrated along the lower edges and corners of the eastern and western walls. Meanwhile, the temperature on the eastern side decreased to around 32°C.By 19:00 (7:00 PM), as solar radiation diminished significantly, the temperature began to drop, with the maximum temperature falling to 43.96°C. The corresponding simulation thermal distribution is illustrated in Figure 1.

Regarding the internal cargo temperature, at 09:00 AM, the maximum temperature was 25.93°C, which was essentially consistent with the ambient temperature. By 12:00 PM, the maximum temperature of the cargo reached 29.17°C, with the hottest area located at the bottom surface in direct contact with the container floor. The temperature on the sun-exposed surfaces of the cargo also began to rise, reaching about 27°C. The internal cargo temperature continued to increase throughout the day, reaching a peak of 38.36°C by 19:00 (7:00 PM). Notably, the highest temperature within the cargo was uniformly distributed across the surfaces exposed to solar radiation. The corresponding simulation results for the cargo temperature are shown in Figure 2.

The simulation, conducted from 08:00 to 19:00 with a constant ambient air temperature of 25°C, yielded the following key findings: External Container Temperature: The container's external temperature exhibited a continuous increase in direct response to the intensifying solar radiation, reaching its peak of approximately 45.52°C around 17:00. Subsequently, as solar radiation diminished, the external surface began to cool. Internal Cargo Temperature: In contrast, the temperature of the internal cargo demonstrated a steady rise from 08:00 onwards. Due to the confined nature of the internal space and the lack of significant airflow exchange, the cargo temperature showed no noticeable decrease by 19:00. A significant cooling phase for the cargo is anticipated to commence only after the container structure itself has cooled sufficiently.

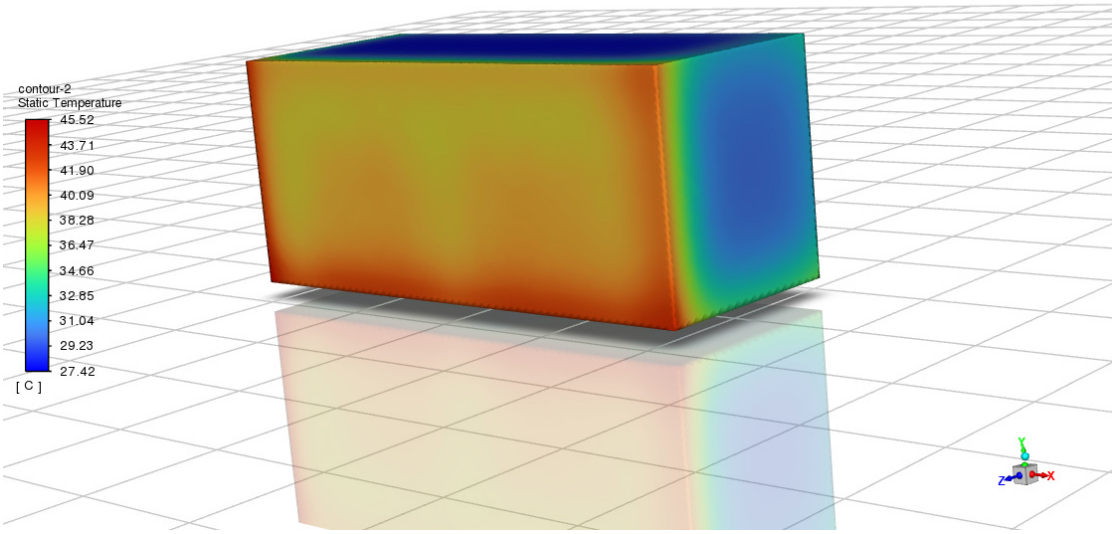

Fig 1. External Wall of Container at 17:00

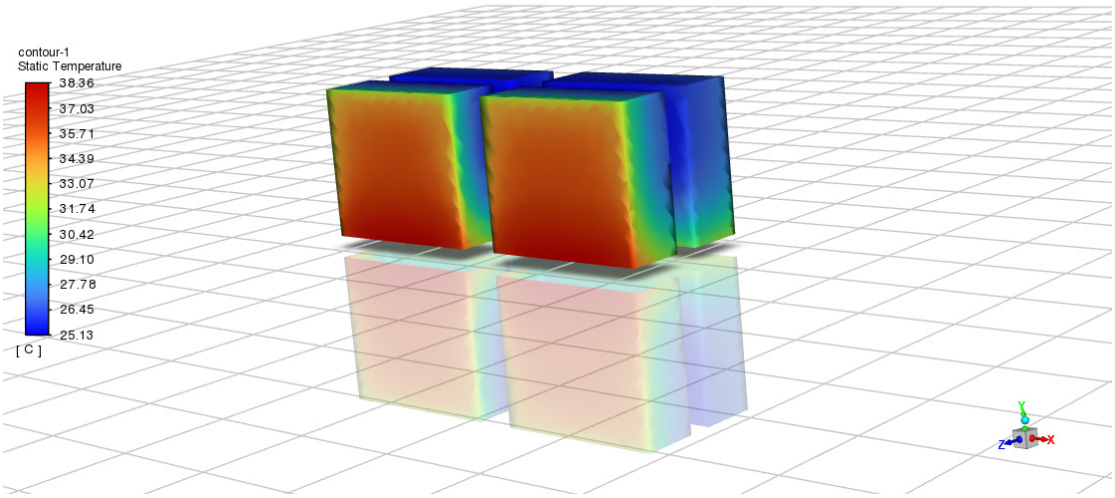

Fig 2. Internal Cargo of Container at 19:00

6. Conclusion

In order to investigate the impact of solar radiation on containers and their cargo in the western plateau region, a 20ft universal container was used as a case study for simulation using Fluent software. The analysis of the effects of plateau solar radiation on containerized goods led to the following conclusion: The modification of the original simulation

model, which applied only solar radiation intensity, by incorporating a solar ray tracing model yields results that align more closely with real-world conditions. Furthermore, the findings are consistent with existing experimental data from previous research.

Future work will focus on refining the ambient temperature data by moving beyond the constraint of a constant temperature, thereby enabling a more thorough investigation of the effects under dynamic temperature variations.

References

[1] Z.K. Yao: Railway Dangerous Goods Transport Safety Risk Analysis and Preventive Measures, Railway Logistics, Vol. 43 (2025) No.7, p.40-43.

[2] Information on http://www.gov.cn/zhengce/zhengceku/2022-01/18/content_5669049.htm.

[3] C.S. Wang, S. Teng and X.H. Wang: Numerical Analysis of Heat Transfer in Dangerous Goods Containers, Journal of the China Railway Society, Vol. 32 (2008) No.1, p.13-18.

[4] Y. Wei: Numerical Simulation of Temperature Field in Dangerous Goods Container (MS., Lanzhou Jiaotong University, China 2015), p.28.

[5] D.C. Ling: Study on Internal Temperature Field of Sea Transport Dangerous Goods Container (MS., Dalian Maritime University, China 2021), p.17.

[6] N. Zou: Research on Safety of Dangerous Goods Container Transport (MS., Lanzhou Jiaotong University, China 2023), p.16.

[7] W.L. Li: Research on Safety Technology for Railway Bulk Sulfur Container Transport (MS., Lanzhou Jiaotong University, China 2024), p.17.

[8] Z.M. Jiang: Simulation Research on Temperature Field of Power Lithium Batteries in Railway Transport (MS., Lanzhou Jiaotong University, China 2023), p.27.

[9] Z.P. Guo, A.K. Kan, C. Meng, et al: Numerical Simulation and Experiment of Temperature Field in Reefer Container, Journal of Shanghai Maritime University, Vol. 38 (2017) No.2, p.82-87.

[10] J.J. Tian, Z. Zhang, M. Li, et al: Experimental Study on Temperature Field Inside Reefer Container, Fluid Machinery, Vol. 44 (2016) No.6, p.56-60.

[11] C.J. Zhao, J.H. Han, X.T. Yang, et al: Numerical Simulation of Spatial Temperature Distribution in Reefer Truck Based on CFD, Transactions of the Chinese Society for Agricultural Machinery, Vol. 44 (2013) No.11, p.168-173.